

Casimir effect in axion electrodynamics with lattice regularizations

Katsumasa Nakayama ^{1,*} and Kei Suzuki ^{2,†}

¹*RIKEN Center for Computational Science, Kobe, 650-0047, Japan*

²*Advanced Science Research Center, Japan Atomic Energy Agency (JAEA), Tokai, 319-1195, Japan*

(Dated: March 6, 2024)

The Casimir effect is induced by the interplay between photon fields and boundary conditions, and in particular, photon fields modified in axion electrodynamics may lead to the sign-flipping of the Casimir energy. We propose a theoretical approach to derive the Casimir effect in axion electrodynamics. This approach is based on a lattice regularization and enables us to discuss the dependence on the lattice spacing for the Casimir energy. With this approach, the sign-flipping behavior of the Casimir energy is correctly reproduced. By taking the continuum limit of physical quantity calculated on the lattice, we can obtain the results consistent with the continuum theory. This approach can also be applied to the Casimir effect at nonzero temperature.

I. INTRODUCTION

The Casimir effect was predicted by Casimir in 1948 [1] and, half a century later, was experimentally confirmed [2, 3] (see Refs. [4–8] for reviews). The conventional Casimir effect means that an attractive force (corresponding to a negative pressure) is induced by quantum fluctuations (particularly, for photon fields in quantum electrodynamics) in space sandwiched by two parallel conducting plates.

Recently, it is expected to be applied to the engineering field such as nanophotonics [9], and the accurate control of the Casimir effect will be an important issue. In particular, the properties of the Casimir effect may be controlled by utilizing topological materials such as Weyl semimetals (WSMs) [10–12] (see Ref. [13] for a review). Inside such materials, the dynamics of photons (i.e., the Maxwell equations) is modified and can be described [14, 15] by the so-called axion electrodynamics [16, 17]. The Casimir effect in axion electrodynamics was studied in Refs. [18–25].¹ In particular, in Ref. [19], one of the most striking findings is a *sign-flipping behavior* of the Casimir energy and also the Casimir force²: there appears not only the well-known negative Casimir energy in a short distance between boundary conditions but also a positive Casimir energy in a long distance. For the application to the engineering field, such a sign-flipping phenomenon depending on the distance will be

useful for controllably switching the attractive, repulsive, and vanishing Casimir force.

In this work, we propose a new and powerful approach to investigate the Casimir effect in axion electrodynamics, which is based on the continuum limit of physical quantities regularized by the lattice space. Our approach with techniques on the lattice will be helpful for future studies because the success of our approach indicates as follows:

- (1): When one investigates the Casimir effect by using lattice gauge simulations of axion electrodynamics, one can correctly simulate the behavior of the Casimir effect in the continuum theory.
- (2): The cutoff effect (namely, the dependence on the lattice spacing) in lattice gauge simulations can be clearly interpreted and safely controlled.
- (3): Using this approach, one can correctly and easily calculate the Casimir energy without carefully dealing with the analytic continuation as in the other approaches.

In fact, approaches using lattice regularizations [43–52] and lattice simulations of gauge fields, such as the U(1) gauge field [53–55], the compact U(1) gauge field [56–60], the SU(2) gauge field [61, 62], and the SU(3) gauge field [63, 64], have been successfully applied and have elucidated the rich physics related to the Casimir effect.

This paper is organized as follows. In Sec. II, we introduce the formulation of the axion electrodynamics and the Casimir effect from its dispersion relations. Section III shows the numerical results of the Casimir energy at zero or nonzero temperatures. The conclusions are in Sec. IV. In Appendices A–D, we provide successful examples of our approach with other models. In Appendix E, we show an example of lattice gauge action simulating the axion electrodynamics in continuous spacetime.

* katsumasa.nakayama@riken.jp

† k.suzuki.2010@th.phys.titech.ac.jp

¹ As a related topic, the photonic Casimir effect in a chiral material was proposed by Jiang and Wilczek [26, 27]. Also, there are many studies on photonic Casimir effects modified by boundary conditions made of topological materials, e.g., between topological insulators [28–31], between Chern insulators [32–34], and between Dirac/Weyl semimetals [22, 24, 35–40] (see Refs. [41, 42] for reviews).

² The Casimir force is defined as the derivative of the Casimir energy with respect to the separation distance.

II. FORMULATION

A. Axion electrodynamics

We first introduce the formulation of the axion electrodynamics in the continuum spacetime [16, 17]. The axion electrodynamics is defined as the U(1) gauge theory with the topological θ term in the 3+1- dimensional spacetime,

$$\mathcal{L} = -\frac{1}{4}F_{\mu\nu}F^{\mu\nu} + \frac{\theta(x)}{4}F_{\mu\nu}\tilde{F}^{\mu\nu}, \quad (1)$$

where $F_{\mu\nu} \equiv \partial_\mu A_\nu - \partial_\nu A_\mu$ is the field-strength tensor with the U(1) gauge field A_μ , and $\tilde{F}^{\mu\nu} \equiv \frac{1}{2}\epsilon^{\mu\nu\alpha\beta}F_{\alpha\beta}$ is the dual tensor. The topological term is characterized by the spacetime-dependent $\theta(x)$. We define the spacetime derivatives of $\theta(x)$ as $b_0 \equiv \partial_t\theta(x)$ and $\mathbf{b} \equiv -\nabla\theta(x)$.³

Throughout this paper, we set $b_0 = 0$ and $\mathbf{b} = (0, 0, b)$. This setup describes time-reversal-symmetry-breaking Weyl semimetals (with a Weyl-node separation b in the z direction) in condensed matter physics or a space-dependent axion-field configuration in high energy physics. On the other hand, the case of $b_0 \neq 0$ and $\mathbf{b} = \mathbf{0}$ describes inversion-symmetry-breaking Weyl semimetals or a time-dependent axion-field configuration. The Casimir effects in the former and latter situations were discussed in Refs. [19–24] and Refs. [18, 23, 25], respectively.

Then, the dispersion relations for photons with the eigenenergy ω_\pm and the three-dimensional momentum (k_x, k_y, k_z) are

$$\omega_\pm^2 = k_x^2 + k_y^2 + \left(\sqrt{k_z^2 + \frac{b^2}{4}} \pm \frac{b}{2} \right)^2. \quad (2)$$

Thus, there are the two branches. Throughout this paper, we call ω_+ and ω_- the *plus mode* and the *minus mode*, respectively. Note that for $b \neq 0$, the plus mode is gapped ($\omega_+ \neq 0$) at any momentum, while the minus mode is gapless ($\omega_- = 0$) at the origin of momentum $(k_x, k_y, k_z) = (0, 0, 0)$.

B. Casimir effect in axion electrodynamics

We impose boundary conditions at $z = 0$ and $z = L_z$, where the z component of momentum is discretized as $k_z \rightarrow \frac{\pi n}{L_z}$ with an integer $n \in \mathbb{Z}$. Such a discretization is

³ A nonzero b_0 is regarded as the chiral chemical potential relevant to the chiral magnetic effect [65–70] as an extra current $j_{\text{CME}} = b_0\mathbf{B}$ parallel to a magnetic field \mathbf{B} . A nonzero \mathbf{b} produces an extra charge $-\mathbf{b}\cdot\mathbf{B}$ relevant to the Witten effect [71] and an extra current $j_{\text{AHE}} = \mathbf{b} \times \mathbf{E}$ in the anomalous Hall effect perpendicular to an electric field \mathbf{E} .

realized with, e.g., the well-known perfectly conducting plate conditions, $E_x = E_y = B_z = 0$.⁴

The zero-point (or vacuum) energy per unit area is represented using the dispersion relation (2),

$$E_0 = \sum_{\pm} \sum_{n=0}^{\infty} \int_{-\infty}^{\infty} \frac{dk_x dk_y}{(2\pi)^2} \frac{\omega_{\pm}}{2}. \quad (3)$$

From this representation, the Casimir energy (per unit area) in axion electrodynamics was derived in Ref. [19]:

$$E_{\text{Cas}} = \frac{b^4 L_z}{16\pi^2} \sum_{m=1}^{\infty} \left[\frac{K_1(mbL_z)}{mbL_z} - \frac{K_2(mbL_z)}{(mbL_z)^2} \right], \quad (4)$$

where K_1 and K_2 are the modified Bessel functions, and the sum over the index $m \in \mathbb{Z}$ is convergent when m is large enough. Since K_1 and K_2 are positive, the positive and negative signs in the first and second terms of Eq. (4) correspond to the repulsive and attractive Casimir forces, respectively. Since the dimension of Eq. (4) is the inverse of length cubed, a dimensionless quantity, which we call the *Casimir coefficient*, is defined as

$$C_{\text{Cas}}^{[3]} \equiv L_z^3 E_{\text{Cas}}, \quad (5)$$

where “[3]” means the exponent of L_z .

C. Thermal Casimir effect in axion electrodynamics

At finite temperature T , the Casimir energy in axion electrodynamics was derived in Ref. [24] using the Lifshitz formula [72] based on the argument principle,

$$E_{\text{Cas}}(T) = T \sum_{\lambda=\pm} \sum'_{l \geq 0} \int_{-\infty}^{\infty} \frac{dk_x dk_y}{(2\pi)^2} \ln \left(1 - e^{-2L_z \tilde{k}_z^{[\lambda, l]}} \right), \quad (6)$$

$$\tilde{k}_z^{[\pm, l]} = \left[\sqrt{\xi_l^2 + k_x^2 + k_y^2} \left(\sqrt{\xi_l^2 + k_x^2 + k_y^2} \mp ib \right) \right]^{\frac{1}{2}}, \quad (7)$$

where $\xi_l \equiv 2\pi Tl$, and the sum over the index l is taken as $\sum'_{l \geq 0} f(l) \equiv f(0)/2 + \sum_{l \geq 1} f(l)$. The integral with respect to k_x and k_y is convergent, so that we can perform numerical integration. For the zero-temperature limit ($T \rightarrow 0$) of the representation (6), we replace as $T \sum'_{l \geq 0} \rightarrow \int_0^{\infty} \frac{d\xi}{2\pi}$, which is equivalent to Eq. (4).

⁴ In the axion electrodynamics, these boundary conditions are not gauge-invariant because of the existence of the θ term. A gauge-invariant boundary condition is considered in Ref. [21], where they obtained the same Casimir energy as that with boundary conditions in Ref. [19].

D. Casimir effect on the lattice

Next, we show the method to calculate the Casimir effect with a lattice regularization [43–52].⁵

The Casimir energy (per unit area) on the lattice with a lattice spacing a is defined as

$$E_{\text{Cas}}^{\text{Lat}} \equiv E_{0+T}^{\text{sum}} - E_{0+T}^{\text{int}}, \quad (8)$$

$$E_{0+T}^{\text{sum}} = \frac{1}{a^3} \sum_{\lambda=+,-} \int_{\text{BZ}} \frac{d(ak_x)d(ak_y)}{(2\pi)^2} \frac{1}{2} \sum_n^{\text{BZ}} \left[\frac{a\omega_{\lambda,n}^{\text{Lat}}}{2} + aT \ln \left(1 - e^{-\frac{1}{T}\omega_{\lambda,n}^{\text{Lat}}} \right) \right], \quad (9)$$

$$E_{0+T}^{\text{int}} = \frac{1}{a^3} \sum_{\lambda=+,-} \int_{\text{BZ}} \frac{d(ak_x)d(ak_y)d(ak_z)}{(2\pi)^3} \left[\frac{a\omega_{\lambda}^{\text{Lat}}}{2} + aT \ln \left(1 - e^{-\frac{1}{T}\omega_{\lambda}^{\text{Lat}}} \right) \right]. \quad (10)$$

The first term of Eq. (8), E_{0+T}^{sum} , is the zero-point and finite-temperature energies made of momenta discretized by a finite length $L_z = aN_z$ (N_z is the number of lattice cells). The second term E_{0+T}^{int} is the energies in infinite volume $L_z \rightarrow \infty$ which is defined by integrals with respect to the three-dimensional momentum. The Casimir energy $E_{\text{Cas}}^{\text{Lat}}$ is defined as the difference between E_{0+T}^{sum} and E_{0+T}^{int} , which is a definition similar to the approach proposed in the original paper by Casimir [1]. The momentum integral is taken within the first Brillouin zone (BZ), and the discrete momenta with the label n are summed over the BZ. When we apply the boundary condition with $ak_z \rightarrow \frac{\pi n}{N_z}$, n is taken as $n = 0, 1, \dots, 2N_z - 1$ (or equivalently $n = 1, 2, \dots, 2N_z$), and the factor $\frac{1}{2}$ in Eq. (9) is required.

For the dispersion relations on the lattice, by substituting $k_i^2 \rightarrow \frac{1}{a^2}(2 - 2 \cos ak_i)$ into Eq. (2), we use⁶

$$(\omega_{\pm}^{\text{Lat}})^2 = \frac{1}{a^2}(2 - 2 \cos ak_x) + \frac{1}{a^2}(2 - 2 \cos ak_y) + \left(\sqrt{\frac{1}{a^2}(2 - 2 \cos ak_z) + \frac{b^2}{4}} \pm \frac{b}{2} \right)^2. \quad (11)$$

⁵ In the present paper, we apply this approach to obtain the continuum limit of physical quantities. Another use is to investigate the Casimir effects originating from degrees of freedom realized on the lattice in solid-state physics, such as electrons, phonons, and magnons, where a is fixed as a constant, and we do not need to take the continuum limit.

⁶ This form can be derived from the leading order of the small a expansion of the action of a lattice gauge field theory with the θ term. See Appendix E. While our discussion is limited within the leading order, numerical simulations of lattice gauge actions, such as Monte Carlo simulations, fully contain the higher-order a effect. In this sense, at a finite a , our prediction of the Casimir effect is more or less different from the results of full numerical lattice simulations. In the continuum limit $a \rightarrow 0$, both should coincide.

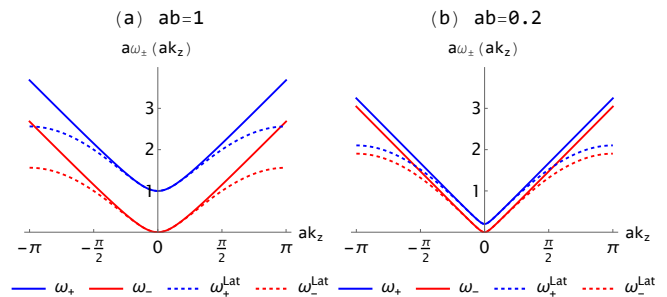


FIG. 1. Dispersion relations for photon fields in axion electrodynamics in the continuum theory characterized by Eq. (2) and a lattice theory defined as Eq. (11). (a) $ab = 1$. (b) $ab = 0.2$.

By multiplying Eq. (8) by L_z^3 , we define a dimensionless Casimir coefficient as

$$C_{\text{Cas}}^{[3]\text{Lat}} \equiv L_z^3 E_{\text{Cas}}^{\text{Lat}} = a^3 N_z^3 E_{\text{Cas}}^{\text{Lat}}. \quad (12)$$

E. Remark on dispersion relations

We remark on the dispersion relations, Eq. (2) for the continuum theory and Eq. (11) for the lattice theory. In Fig. 1, we compare these dispersion relations for the k_z direction on a coarser lattice of $ab = 1$ and for a finer lattice of $ab = 0.2$ (ab is dimensionless). For example, let us consider a fixed $b = 1$ (b is dimensional). If $a = 1$, the minus modes from the two theories agree with each other in the region of $\omega_- \sim \omega_-^{\text{Lat}} < 0.5$, equivalently $a\omega_- \sim a\omega_-^{\text{Lat}} < 0.5$ [see Fig. 1(a)], whereas if $a = 0.2$, $\omega_- \sim \omega_-^{\text{Lat}} < 2.5$, equivalently $a\omega_- \sim a\omega_-^{\text{Lat}} < 0.5$ [see Fig. 1(b)]. Thus, as long as the dimensionless quantity ab is smaller, the approximation of the low-energy/low-momentum modes in ω_{\pm} by using $\omega_{\pm}^{\text{Lat}}$ is better. This suggests that the continuum limit ($a \rightarrow 0$) of the lattice theory serves as a precise estimate of the Casimir effect if the Casimir effect is dominated by the contributions from low-energy/low-momentum modes. In the next section, we numerically examine this discussion.

III. RESULTS

A. Zero temperature

In Fig. 2, we show the numerical results of the Casimir coefficients, defined as Eq. (5) in the continuum theory and Eq. (12) in the lattice theory. In a short distance, we find a negative Casimir energy corresponding to an attractive Casimir force, which is similar to the Casimir effect in the usual photon field characterized by $b = 0$. In particular, at $bL_z = 0$, $C_{\text{Cas}}^{[3]} = -\frac{\pi^2}{720} \sim -0.0137$, which is well known as the result for the normal photon field in

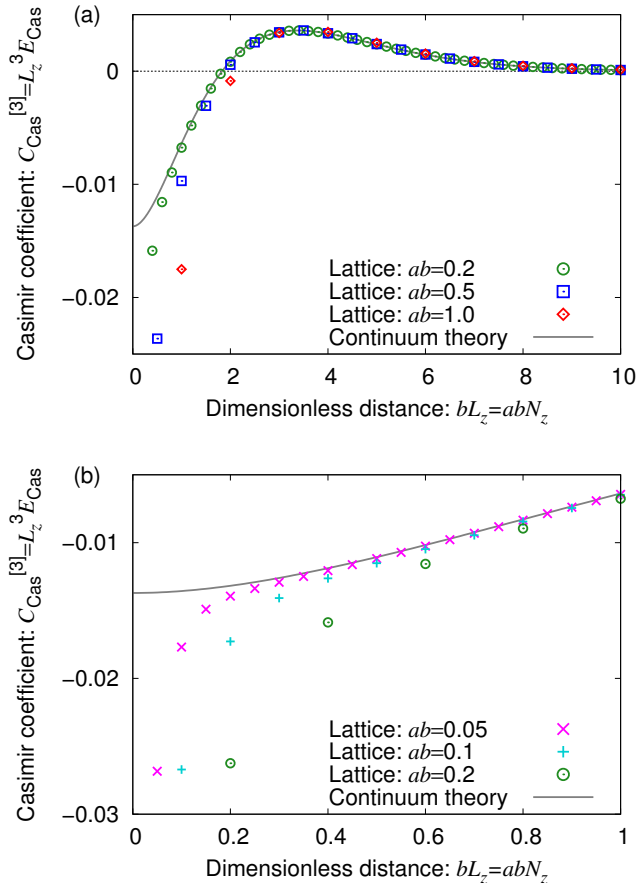


FIG. 2. Casimir coefficients in axion electrodynamics at zero temperature. The solid line and the points are the results in the continuum and lattice theories, respectively. (a) $bL_z \leq 10$. (b) $bL_z \leq 1$.

the continuum theory (also see Appendix A). The sign of the Casimir energy flips at $bL_z \simeq 2$, and in a long distance, a positive Casimir energy corresponding to a repulsive Casimir force appears, which is a feature in axion electrodynamics with $\mathbf{b} \neq \mathbf{0}$ and $b_0 = 0$ [19].⁷ This tendency holds in both continuum theory (plotted as the solid line) and lattice theories discretized by lattice spacing a (plotted as the points).

In the lattice theory, we can investigate lattice spacing a dependence. In the positive-Casimir-energy region, $bL_z \gtrsim 2$, the lattice theory at $ab = 0.5$ is already consistent with the continuum theory. In the negative-Casimir-energy region, $bL_z \lesssim 2$, the a dependence is enhanced due to an ultraviolet lattice cutoff effect (namely, a lattice ar-

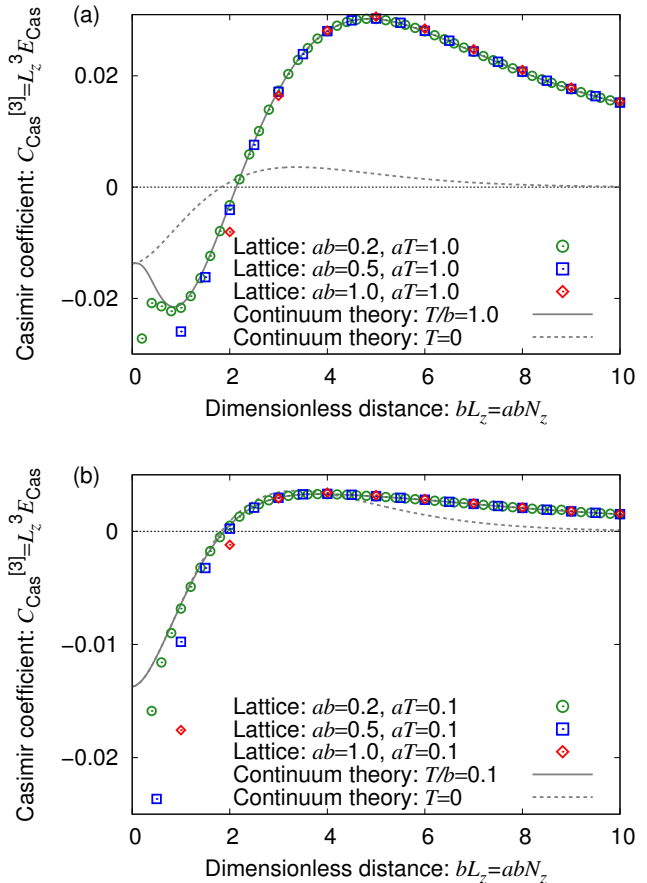


FIG. 3. Casimir coefficients in axion electrodynamics at finite temperature. (a) $aT = 1.0$. (b) $aT = 0.1$.

tifact), but the result agrees with that in the continuum theory by taking smaller lattice spacing. Thus, the continuum limit from a lattice theory can correctly reproduce the exact solution in the continuum theory. This is evidence that a lattice regularization scheme is useful for investigating the Casimir effect in axion electrodynamics.

Note that the qualitative behavior of the sign flipping does not change even when we replace the current boundary conditions with the periodic boundary conditions (see Appendix B). Also, the existence of the momenta (k_x and k_y) perpendicular to \mathbf{b} is crucial. We can discuss it with the two- or one-dimensional analogous model (see Appendix C).

B. Finite temperature

In Fig. 3, we show the numerical results at nonzero temperatures, $aT = 1$ and 0.1 . Even at finite temperatures, we find the sign-flipping behavior of the Casimir

⁷ The sign-flipping points of the Casimir energy (equivalently, Casimir coefficient) and the Casimir force are slightly off. This is because the Casimir force is defined as $F_{\text{Cas}} \equiv -\frac{\partial}{\partial L_z} E_{\text{Cas}}$. Therefore, the sign-flipping point of F_{Cas} corresponds to the extremum of E_{Cas} : $bL_z \simeq 2.38$ [19]. Note that the extrema of E_{Cas} and $C_{\text{Cas}}^{[3]}$ are also slightly off.

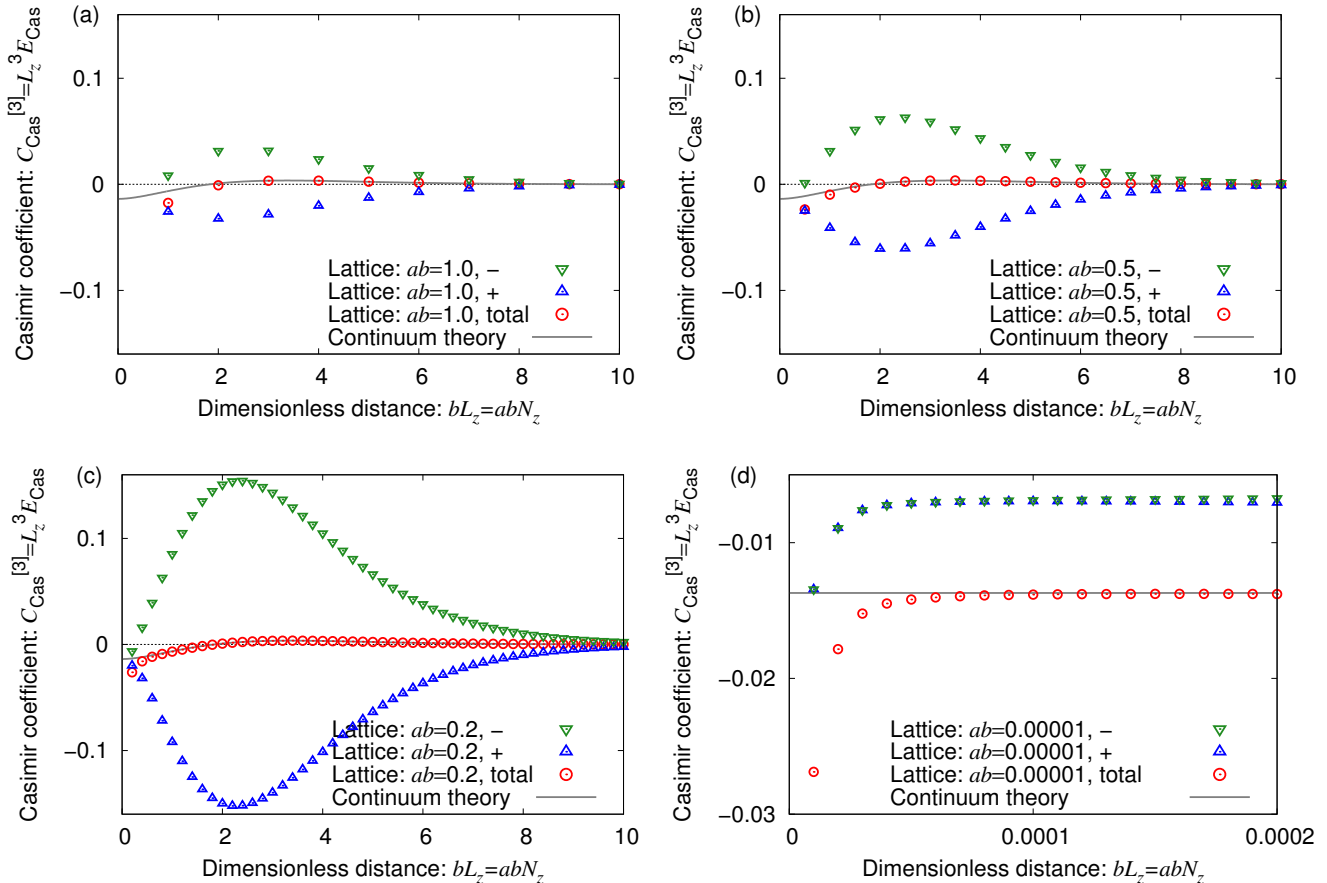


FIG. 4. Contributions from the plus/minus modes in Casimir coefficients in axion electrodynamics at zero temperature. (a)-(c) $ab = 1.0, 0.5,$ and 0.2 within $bL_z \leq 10$. (b) $ab = 0.00001$.

energy at $bL_z \sim 2$.⁸ Low temperature ($aT = 0.1$) mainly contributes to the infrared positive-Casimir-energy region in a long distance $bL_z \gtrsim 2$. High temperature ($aT = 1.0$) contributes to also the ultraviolet negative-Casimir-energy region in a short distance $bL_z \lesssim 2$. Although the ultraviolet region has a large a dependence similar to the zero-temperature case, we can safely reproduce the continuum result by taking the continuum limit $a \rightarrow 0$. This is also evidence that a lattice regularization scheme is useful for investigating the Casimir effect even at finite temperature.

C. Anatomy of plus/minus modes

As seen in Eq. (2) [and also Eq. (11) on the lattice], the dispersion relations of the plus and minus modes are different from each other, so that in general each mode

should induce a different contribution. One of the questions here is how much each mode contributes to the Casimir effect in axion electrodynamics.

Using regularization approaches in prior studies, such as a zeta-function regularization and the Lifshitz formula,⁹ we can prove that each mode gives half of the total Casimir energy: There is no difference between the plus-mode and minus-mode contributions.

In this section, we investigate this question by using our lattice regularization. In Fig. 4, we plot the results for the plus and minus modes separately and compare them and the sum of the two modes. At $ab = 1$ in Fig. 4(a), we find that the signs of contributions from the two modes are opposite. After summing the two modes, the sign of the total Casimir energy is determined (negative in the short distance and positive in the long distance).

However, this is not our conclusion. As shown in Figs. 4(b) and (c), we find that each contribution de-

⁸ Note that in Fig. 3(a), we also see the extremum of $C_{\text{Cas}}^{[3]}$ near $bL_z \sim 1$. However, this is not the extremum of E_{Cas} , and hence the sign of the Casimir force does not flip in this region.

⁹ Since the zero-point energy consists of the sum of the plus and minus modes [as in Eq. (3)], one can apply a regularization approach to each mode separately.

depends on ab , while the total result is independent of ab . Such relevant a dependence suggests that although each contribution is not sufficiently regularized within our lattice regularization, the total Casimir energy is correctly regularized.

Furthermore, as shown in Figs. 4(d), if we focus on a tiny ab , the contributions from the plus and minus modes are almost the same, and hence the total Casimir energy is interpreted as twice each contribution, which is consistent with the picture in the continuum theory. Thus, the failure of our lattice regularization is limited to the intermediate ab region.

In this work, our lattice regularization is defined as the form of the dispersion relations (11) on the lattice. In order to improve our lattice regularization, it might be better to transform Eq. (11) into an appropriate form.

IV. CONCLUSIONS

In this paper, we showed that the sign-flipping behavior of the Casimir effect in axion electrodynamics can be derived with a lattice regularization, which is consistent with the continuum theory.

Our approach can be successfully applied not only to the standard axion electrodynamics but also to other models. For example, we can check the consistency with the continuum theory for the massive scalar field (Appendix A), the case of the periodic boundary condition (Appendix B), lower-dimension models (Appendix C), and photon fields modified in chiral media (Appendix D). Thus, our approach is basically successful, but in Sec. III C, we showed an example of inconsistency with the continuum theory. Such inconsistency may suggest that the regularization is insufficient and might be improved by introducing a modified lattice regularization, which is left for future studies.

ACKNOWLEDGMENTS

The authors thank Maxim N. Chernodub for providing information on Weyl semimetals and lattice Yang-Mills simulations. K. S. also appreciates the fruitful discussions in the informal meeting at JAEA. This work was supported by the Japan Society for the Promotion of Science (JSPS) KAKENHI (Grant No. JP20K14476).

Appendix A: Massive scalar field

In this Appendix, in order to check the applicability of our approach with a lattice regularization, we demonstrate the Casimir effect for a massive real scalar field, where the dispersion relation with a mass M in the $d+1$ dimensional spacetime is given as

$$(\omega^{\text{mass}})^2 = k_x^2 + k_y^2 + k_z^2 + \cdots + k_{x_d}^2 + M^2. \quad (\text{A1})$$

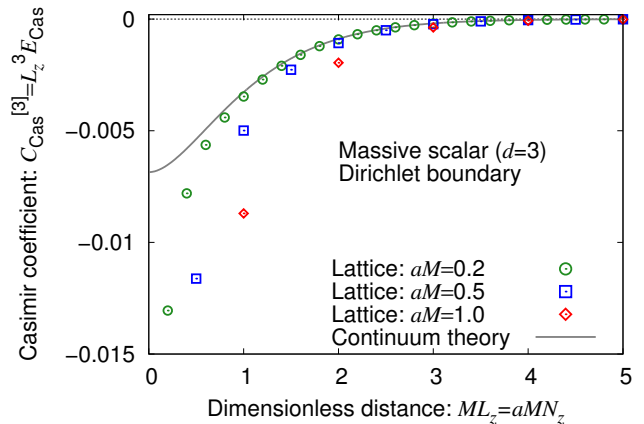


FIG. 5. Casimir coefficients for massive scalar fields in the 3+1-dimensional spacetime with the Dirichlet boundary condition.

In the continuum theory, the Casimir energy (per unit area) with the boundary condition with $k_z \rightarrow \frac{\pi n}{L_z}$ for the z direction is obtained as [73, 74]

$$E_{\text{Cas}}^{\text{mass}} = -\frac{2}{(4\pi)^{(d+1)/2}} \frac{M^{(d+1)/2}}{L_z^{(d-1)/2}} \sum_{m=1}^{\infty} \frac{K_{(d+1)/2}(2mML_z)}{m^{(d+1)/2}}. \quad (\text{A2})$$

When we take the massless limit $M \rightarrow 0$, this formula can reproduce the results for the massless real scalar field, $E_{\text{Cas}} = -\frac{\pi}{24L_z}$, $-\frac{\zeta(3)}{16\pi L_z^2}$, and $-\frac{\pi^2}{1440L_z^3}$ at $d = 1, 2$, and 3 , respectively.¹⁰

In addition, we remark on the relationship between the Casimir effects for the massive field and in axion electrodynamics. When we fix $d = 3$ and replace as $M \rightarrow \frac{b}{2}$, Eq. (A2) agrees with the second term of Eq. (4) for the Casimir energy in axion electrodynamics, except for the factor 1/2 due to degrees of freedom for polarizations. Thus, the solution (4) contains the behavior of the Casimir effect for massive fields, and particularly the short-distance behavior is dominated by it. While the second term of Eq. (4) can be simply interpreted as a massive-field-like Casimir effect, the first term leads to novel effects such as the sign-flipping behavior and the repulsive Casimir force.

In Fig. 5, we compare the numerical results from the lattice regularization and Eq. (A2) at $d = 3$. The result from the lattice theory with a small lattice spacing well agrees with that from the continuum theory.

¹⁰ An analytic solution for the massless real scalar field is [Eq. (2.13) in Ref. [73]]

$$E_{\text{Cas}}^{\text{mass}}(M \rightarrow 0) = -(4\pi)^{-\frac{(d+1)}{2}} \Gamma\left(\frac{d+1}{2}\right) \frac{\zeta(d+1)}{L_z^d}. \quad (\text{A3})$$

Note that the result for $d = 1$ in Eq. (2.15) of Ref. [73] includes a typo.

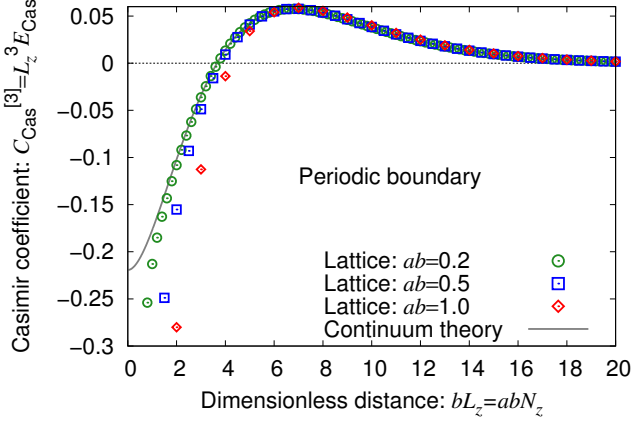


FIG. 6. Casimir coefficients in axion electrodynamics with the periodic boundary condition.

Appendix B: Periodic boundary condition

While in the main text, we focus on the boundary condition with $k_z \rightarrow \frac{\pi n}{L_z}$, in this Appendix, we show the periodic boundary condition (PBC). Note that the Casimir effect with the PBC for one spatial dimension is physical in the solid-torus type of material, where the usual Casimir force (as in the parallel-plates geometry) cannot be observed, but the internal pressure and the internal energy density can be modified by the Casimir energy. Furthermore, when one simulates the Casimir effect in numerical lattice gauge simulations, simulations with the PBC will be helpful as a simple condition.

The zero-point energy in the PBC is

$$E_0^{\text{PBC}} = \sum_{\pm} \sum_{n=-\infty}^{\infty} \int_{-\infty}^{\infty} \frac{dk_x dk_y}{(2\pi)^2} \frac{\omega_{\pm}^{\text{PBC}}}{2}. \quad (\text{B1})$$

The differences from the case of Eq. (3), are (i) the summation range (from $-\infty$ to ∞) over n and (ii) the discrete momentum $k_z \rightarrow \frac{2\pi n}{L_z}$ in the dispersion relation $\omega_{\pm}^{\text{PBC}}$. By using the definition of the zero-point energy and an appropriate regularization scheme, we obtain the Casimir energy as

$$E_{\text{Cas}}^{\text{PBC}} = \frac{b^4 L_z}{16\pi^2} \sum_{m=1}^{\infty} \left[\frac{K_1(mbL_z/2)}{mbL_z/2} - \frac{K_2(mbL_z/2)}{(mbL_z/2)^2} \right]. \quad (\text{B2})$$

This form can also be obtained by replacing L_z in Eq. (4) with $L_z/2$ and by multiplying the whole by the factor 2. For the definition of the Casimir energy in the lattice theory with the PBC, we need to remove the factor $\frac{1}{2}$ in Eq. (9), which is caused by the range of n in Eq. (B1).

In Fig. 6, we show the numerical results from the continuum and lattice theories. Thus, the magnitude of the Casimir energy with the PBC is larger than that with the boundary condition with $k_z \rightarrow \frac{\pi n}{L_z}$ (see Fig. 2), but

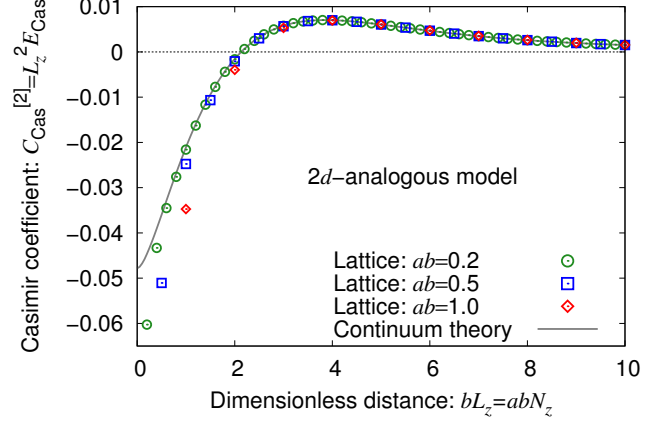


FIG. 7. Casimir coefficients in a two-dimension analogous model for axion electrodynamics.

the qualitative behavior does not change. Therefore, our result suggests that lattice simulations of axion electrodynamics with the PBC can reproduce the sign-flipping behavior of the Casimir energy.

Appendix C: Two-dimensional analogous model

While the usual axion electrodynamics is defined in the $3+1$ dimensional spacetime, it is instructive to consider lower-dimension analogous theories, such as $2+1$ - and $1+1$ -dimensions, where we define the following dispersion relations:

$$(\omega_{\pm}^{2d})^2 = k_x^2 + \left(\sqrt{k_z^2 + \frac{b^2}{4}} \pm \frac{b}{2} \right)^2, \quad (\text{C1})$$

$$(\omega_{\pm}^{1d})^2 = \left(\sqrt{k_z^2 + \frac{b^2}{4}} \pm \frac{b}{2} \right)^2. \quad (\text{C2})$$

From Eq. (C1) and the Lifshitz formula, the Casimir energy in the $2+1$ -dimensional continuum theory with the boundary condition with $k_z \rightarrow \frac{\pi n}{L_z}$ for the z direction is obtained as

$$E_{\text{Cas}}^{2d} = \sum_{\lambda=\pm} \int_0^{\infty} \frac{d\xi}{2\pi} \int_{-\infty}^{\infty} \frac{dk_x}{2\pi} \ln \left(1 - e^{-2L_z \tilde{k}_z^{[\lambda]}} \right), \quad (\text{C3})$$

$$\tilde{k}_z^{[\pm]} \equiv \left[\sqrt{\xi^2 + k_x^2} \left(\sqrt{\xi^2 + k_x^2} \mp ib \right) \right]^{\frac{1}{2}}. \quad (\text{C4})$$

The Casimir coefficient is defined as $C_{\text{Cas}}^{[2]} \equiv L_z^2 E_{\text{Cas}}$.

In Fig. 7, we compare the solution of Eq. (C3) in the continuum theory and the numerical results with the lattice regularization. Thus, the Casimir effect in the $2+1$ -dimensional model is analogous to that in the usual axion electrodynamics.

We note that the dispersion relation in the $1+1$ -dimensional model defined as Eq. (C2) is similar to the

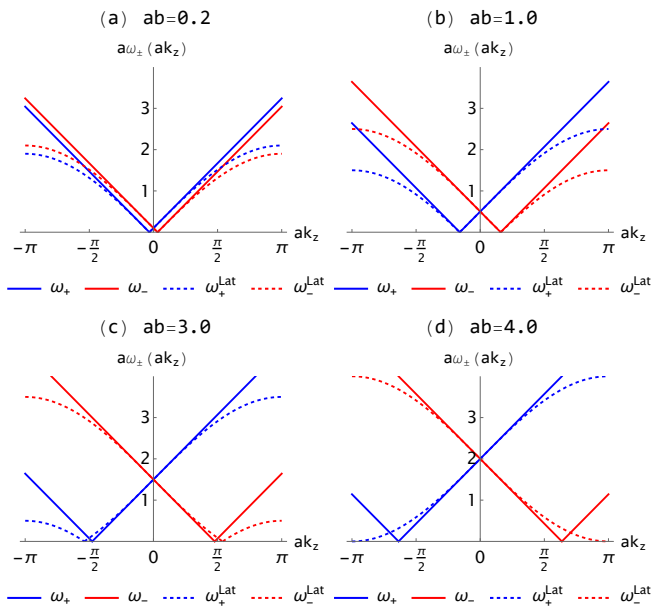


FIG. 8. Dispersion relations for photon fields in the Jiang-Wilczek model in the continuum theory characterized by Eq. (D1) and a lattice theory defined as Eq. (D3). (a) $ab = 0.2$. (b) $ab = 1.0$. (c) $ab = 3.0$. (d) $ab = 4.0$.

massive field, except for the constant energy shift of $\pm \frac{b}{2}$. Because the constant term $\pm \frac{b}{2}$ does not contribute to the Casimir energy, the Casimir energy in this model is completely the same as that in the massive field theory with the dispersion relation $\omega = \sqrt{k_z^2 + b^2/4}$. Thus, the Casimir effect in this 1+1-dimensional model is not analogous to that in the usual axion electrodynamics. This is because there is no momentum perpendicular to the compactified direction in the dispersion relation (C2).

Appendix D: Jiang-Wilczek model

In Ref. [26] (also see Ref. [27]), Jiang and Wilczek investigated the Casimir effect for photons in chiral media showing the Faraday effect or the optical activity. In their model, the dispersion relations of photons are different from those in axion electrodynamics, and hence the qualitative behavior of the Casimir effect is also different: The sign-flipping behavior occurs not once but infinitely many times: the Casimir energy oscillates. In this Appendix, we demonstrate this effect from the lattice regularization.

The dispersion relations in the continuum theory are

$$(\omega_{\pm}^{\text{JW}})^2 = k_x^2 + k_y^2 + \left(k_z \pm \frac{b}{2}\right)^2. \quad (\text{D1})$$

This expression formally means that the two (normal) linear dispersion relations are shifted by $\pm \frac{b}{2}$ in the k_z direction, where we call Eq. (D1) the *Jiang-Wilczek model*.

Note that in Ref. [26], the constant b is related to the parameters of the Faraday effect (the magnitude of a magnetic field and the Verdet constant) or the parameters of an optically active material. From Eq. (D1), the Casimir energy in the continuum theory is obtained as [26]

$$E_{\text{Cas}}^{\text{JW}} = \int_0^\infty \frac{d\xi}{2\pi} \int_{-\infty}^\infty \frac{dk_x dk_y}{(2\pi)^2} \ln \left[1 + e^{-4\sqrt{\xi^2 + k_x^2 + k_y^2} L_z} - 2e^{-2\sqrt{\xi^2 + k_x^2 + k_y^2} L_z} \cos(bL_z) \right]. \quad (\text{D2})$$

For dispersion relations with the lattice regularization, we apply the following forms:

$$(\omega_{\pm}^{\text{LatJW}})^2 = \frac{1}{a^2} (2 - 2 \cos ak_x) + \frac{1}{a^2} (2 - 2 \cos ak_y) + \left(\frac{2}{a} \sin \frac{ak_z}{2} \pm \frac{b}{2} \right)^2. \quad (\text{D3})$$

In Fig. 8, we show the dispersion relations in the continuum and lattice theories. Thus, when ab is small enough, the structure near $k_z = \pm \frac{b}{2}$ (namely, the structure like the separated Weyl points) is well approximated by the lattice theory.

Note that when we apply Eq. (D3), the first BZ for ak_z is not $0 \leq ak_z < 2\pi$ but $0 \leq ak_z < 4\pi$. Then, for the definition of the Casimir energy, we have to replace as $\frac{1}{2} \sum_n^{\text{BZ}} \rightarrow \frac{1}{4} \sum_n^{\text{BZ}}$ in Eq. (9) and $\int_{\text{BZ}} \frac{d(ak_z)}{2\pi} \rightarrow \int_{\text{BZ}} \frac{d(ak_z)}{4\pi}$ in Eq. (10).

In Fig. 9(a), we show the numerical results for $ab = 0.2$ and 1.0 to check the validity of the lattice regularization. We find that the oscillatory behavior at $ab = 0.2$ is clearly consistent with that in the continuum theory, except for the smallest bL_z . Thus, this lattice regularization approach can be safely applied to an “oscillating” Casimir effect. Even at $ab = 1.0$, we find that the oscillation almost agrees with the continuum theory, but precisely speaking, it is slightly modified. Such a modification suggests that the Weyl-points-like structure is slightly different from the continuum theory [See Fig. 8(b)].

To comprehensively examine artifacts caused by a coarser lattice spacing a (or equivalently a larger b effect), in Fig. 9(b), we also show the results at $ab = 3.0$ and 4.0. At $ab = 3.0$, we find that the amplitude of oscillation is suppressed, compared to the continuum theory. This is due to a large lattice artifact near the Weyl-points-like structure [See Fig. 8(c)]. At $ab = 4.0$, the amplitude becomes almost zero, except for the smallest bL_z . This is because, at $ab = 4.0$, the Weyl-points-like structure in the lattice dispersion relations completely disappears [See Fig. 8(d)]. Thus, when a or b is large enough, the current lattice regularization cannot approximate the continuum theory, and hence the similar Casimir effect cannot be reproduced.

Appendix E: Lattice field theory

In the main text, we assumed the dispersion relations of photon fields on the lattice, Eq. (11). Eq. (11) can be

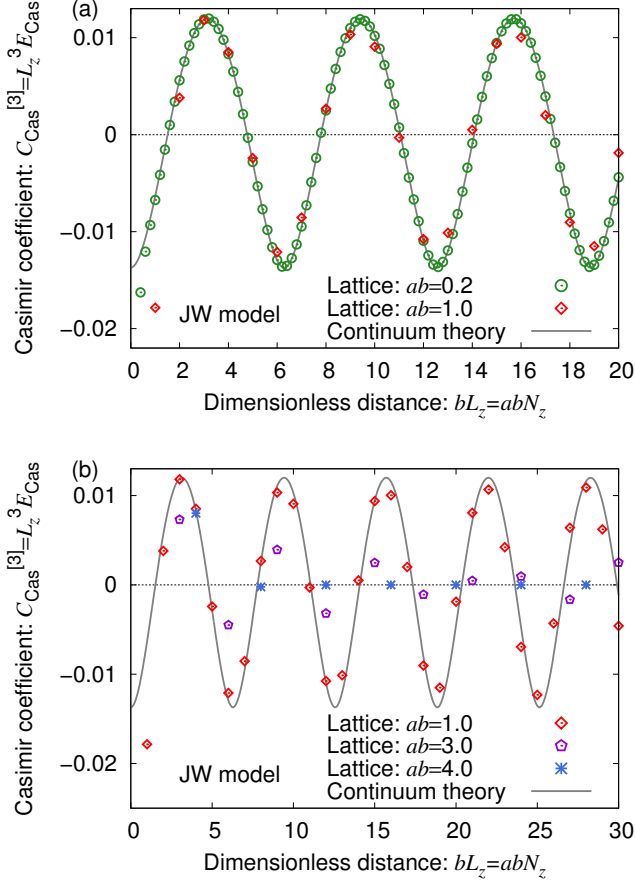


FIG. 9. Casimir coefficients in the Jiang-Wilczek model. (a) $ab = 0.2$ and 1.0 . (b) $ab = 1.0, 3,$ and 4 .

interpreted as an ansatz for the regularization to calculate the Casimir energy, while it can be derived from a lattice gauge field theory.

In this appendix, we provide a derivation of the dispersion relations of the U(1) gauge field in an axion electrodynamics on the lattice. We consider a total action in the four-dimensional Euclidean space, defined as

$$S_{\text{tot}} \equiv S_{\text{Wil}} + S_{\theta} + S_{\xi}, \quad (\text{E1})$$

where S_{Wil} is the Wilson plaquette action [75], S_{θ} is the action of the topological θ term, and S_{ξ} is the action for the gauge fixing. From this action, we will derive the inverse propagator $G_{\mu\nu}^{-1}$ for the U(1) gauge field A_{μ} , defined as

$$S_{\text{tot}} = -\frac{a^4}{2} \sum_n A_{\mu} G_{\mu\nu}^{-1} A_{\nu}, \quad (\text{E2})$$

where n is the label of lattice sites on the Euclidean space.

First, we define the gauge-invariant plaquette $U_{\mu\nu}$ as

$$\begin{aligned} U_{\mu\nu}(n) &= e^{iag[A_{\mu}(n+\hat{\mu}/2)+A_{\nu}(n+\hat{\mu}+\hat{\nu}/2)]} \\ &\quad \times e^{-iag[A_{\mu}(n+\hat{\nu}+\hat{\mu}/2)+A_{\nu}(n+\hat{\nu}/2)]} \\ &= e^{ia^2g(\nabla_{\mu}A_{\nu}(n_c) - \nabla_{\nu}A_{\mu}(n_c))}, \end{aligned} \quad (\text{E3})$$

where a and g are the lattice spacing and the coupling constant, respectively. Here, $n_c \equiv n + \hat{\mu}/2 + \hat{\nu}/2$ is the central point of a square lattice. With the plaquette $U_{\mu\nu}$, we can define the Wilson plaquette gauge action [75] as follows:

$$\begin{aligned} S_{\text{Wil}} &= -\frac{1}{2g^2} \sum_{n,\mu<\nu} 2\text{Re tr } U_{\mu\nu}(n) \\ &= -\frac{1}{4g^2} \sum_n [2 - a^4g^2(\nabla_{\mu}A_{\nu}(n_c) - \nabla_{\nu}A_{\mu}(n_c))^2 + O(a^6)]. \end{aligned} \quad (\text{E4})$$

For the calculation of $(\nabla_{\mu}A_{\nu}(n_c) - \nabla_{\nu}A_{\mu}(n_c))^2$ in Eq. (E4), we use the following equation

$$\begin{aligned} \sum_n (\nabla_{\mu}A_{\nu}(n_c))(\nabla_{\rho}A_{\sigma}(n_c)) &= \sum_n (A_{\nu}(n_c + \hat{\mu}/2) - A_{\nu}(n_c - \hat{\mu}/2))(A_{\sigma}(n_c + \hat{\rho}/2) - A_{\sigma}(n_c - \hat{\rho}/2)) \\ &= -\sum_n A_{\nu}(n_c + \hat{\mu}/2) [\nabla_{\mu}(A_{\sigma}(n_c + \hat{\rho}/2 + \hat{\mu}/2) - A_{\sigma}(n_c - \hat{\rho}/2 + \hat{\mu}/2))] \\ &= -\sum_n A_{\nu}(n_c + \hat{\mu}/2) [\nabla_{\rho}\nabla_{\mu}(A_{\sigma}(n_c + \hat{\mu}/2))], \end{aligned} \quad (\text{E5})$$

where we set $(\rho, \sigma) = (\mu, \nu)$ or $(\rho, \sigma) = (\nu, \mu)$. When we ignore the constant term and $O(a^6)$ contributions in Eq. (E4), we finally get the leading order of the Wilson plaquette action which corresponds to $\int d^4x \frac{1}{4} F_{\mu\nu} F_{\mu\nu}$ in

the continuum theory,

$$S_{\text{Wil}} \simeq -\frac{a^4}{2} \sum_n A_{\mu} (\delta_{\mu\nu} \nabla^2 - \nabla_{\mu} \nabla_{\nu}) A_{\nu}. \quad (\text{E6})$$

Next, we consider a topological θ term on the lattice [76, 77], which corresponds to $\int d^4x \frac{i\theta}{4} F_{\mu\nu} \tilde{F}_{\mu\nu}$ in the continuum theory.

$$\begin{aligned} S_\theta &= -\frac{i\theta}{8g^2} \sum_n \epsilon_{\mu\nu\rho\sigma} \text{tr}[U_{\mu\nu} U_{\rho\sigma}] \\ &= -\frac{i\theta}{8g^2} \sum_n \epsilon_{\mu\nu\rho\sigma} [1 + ia^2 g(\nabla_\mu A_\nu - \nabla_\nu A_\mu)] \\ &\quad \times [1 + ia^2 g(\nabla_\rho A_\sigma - \nabla_\sigma A_\rho)] + O(a^6). \end{aligned} \quad (\text{E7})$$

By ignoring the constant term and the $O(a^6)$ contributions, we get

$$\begin{aligned} S_\theta &\simeq \frac{i\theta a^4}{2} \sum_n (\nabla_\mu A_\nu) \left[\frac{1}{2} \epsilon_{\mu\nu\rho\sigma} (\nabla_\rho A_\sigma - \nabla_\sigma A_\rho) \right] \\ &= \frac{-i\nabla_z \theta a^4}{2} \epsilon_{z\nu\rho\sigma} \sum_n A_\nu \nabla_\rho A_\sigma \\ &= \frac{iba^4}{2} \epsilon_{z\nu\rho\sigma} \sum_n A_\nu \nabla_\rho A_\sigma + O(a^6), \end{aligned} \quad (\text{E8})$$

where we used the definition $b \equiv -\partial_z \theta$ for the leading part of $-\nabla_z \theta = -\partial_z \theta + O(a^2)$.

We also consider the gauge fixing term $-\int d^4x \frac{1}{2\xi} (\partial_\mu A_\mu)^2$. On the lattice, it is discretized

as $\partial_\mu A_\mu \rightarrow \nabla_\mu A_\mu$:

$$S_\xi \simeq -\frac{a^4}{2\xi} \sum_n (\nabla_\mu A_\mu)^2. \quad (\text{E9})$$

Since the gauge fixing term does not contribute to the calculation of the gauge invariant physical quantities, we add this term to match our perturbative representation to the conventional representation of the continuum theory.¹¹

Note that the ghost field does not contribute to the Casimir effect because of the cancellation with the contribution from the longitudinal photons (see Ref. [19] for the axion electrodynamics in the continuum spacetime).

By gathering Eq. (E6), (E8), and (E9), we get the inverse propagator on the lattice as follows:

$$G_{\mu\nu}^{-1} = \delta_{\mu\nu} \nabla^2 + i\epsilon_{\mu\nu z\sigma} b \nabla_\sigma - (1 - \xi^{-1}) \nabla_\mu \nabla_\nu. \quad (\text{E10})$$

By the replacement of $\nabla_\mu \rightarrow \partial_\mu$, we find the corresponding inverse propagator in the continuum theory. To move on to the momentum space, we substitute $a\nabla_\mu \rightarrow -i \sin(ak_\mu/2)$. It means that all the momenta k_μ in the continuum theory are replaced by the momenta on the lattice, $\sin(ak_\mu/2)$.

Then, by substituting $\sin(ak_\mu/2)$ into the dispersion relations (2) for photons in the continuum spacetime, we find the lattice representation of the dispersion relations (11).

-
- [1] H. B. G. Casimir, On the Attraction Between Two Perfectly Conducting Plates, Proc. Kon. Ned. Akad. Wetensch. **51**, 793 (1948).
- [2] S. K. Lamoreaux, Demonstration of the Casimir Force in the 0.6 to $6\mu\text{m}$ Range, *Phys. Rev. Lett.* **78**, 5 (1997), [Erratum: *Phys. Rev. Lett.* **81**, 5475 (1998)].
- [3] G. Bressi, G. Carugno, R. Onofrio, and G. Ruoso, Measurement of the Casimir force between parallel metallic surfaces, *Phys. Rev. Lett.* **88**, 041804 (2002), arXiv:quant-ph/0203002.
- [4] G. Plunien, B. Müller, and W. Greiner, The Casimir Effect, *Phys. Rep.* **134**, 87 (1986).
- [5] V. M. Mostepanenko and N. N. Trunov, The Casimir Effect and Its Applications, *Sov. Phys. Usp.* **31**, 965 (1988).
- [6] M. Bordag, U. Mohideen, and V. M. Mostepanenko, New developments in the Casimir effect, *Phys. Rep.* **353**, 1 (2001), arXiv:quant-ph/0106045 [quant-ph].
- [7] K. A. Milton, *The Casimir Effect: Physical Manifestations of Zero-Point Energy* (World Scientific, Singapore, 2001).
- [8] G. L. Klimchitskaya, U. Mohideen, and V. M. Mostepanenko, The Casimir force between real materials: Experiment and theory, *Rev. Mod. Phys.* **81**, 1827 (2009), arXiv:0902.4022 [cond-mat.other].
- [9] T. Gong, M. R. Corrado, A. R. Mahbub, C. Shelden, and J. N. Munday, Recent progress in engineering the Casimir effect – applications to nanophotonics, nanomechanics, and chemistry, *Nanophotonics* **10**, 523 (2021).
- [10] X. Wan, A. M. Turner, A. Vishwanath, and S. Y. Savrasov, Topological semimetal and Fermi-arc surface states in the electronic structure of pyrochlore iridates, *Phys. Rev. B* **83**, 205101 (2011), arXiv:1007.0016 [cond-mat.str-el].
- [11] K.-Y. Yang, Y.-M. Lu, and Y. Ran, Quantum Hall effects in a Weyl semimetal: Possible application in pyrochlore iridates, *Phys. Rev. B* **84**, 075129 (2011), arXiv:1105.2353 [cond-mat.str-el].
- [12] A. A. Burkov and L. Balents, Weyl Semimetal in a Topological Insulator Multilayer, *Phys. Rev. Lett.* **107**, 127205 (2011), arXiv:1105.5138 [cond-mat.mes-hall].
- [13] N. P. Armitage, E. J. Mele, and A. Vishwanath, Weyl and Dirac Semimetals in Three Dimensional Solids, *Rev. Mod. Phys.* **90**, 015001 (2018), arXiv:1705.01111 [cond-mat.str-el].
- [14] A. G. Grushin, Consequences of a condensed matter realization of Lorentz violating QED in Weyl semi-metals, *Phys. Rev. D* **86**, 045001 (2012), arXiv:1205.3722 [hep-th].
- [15] A. A. Zyuzin and A. A. Burkov, Topological response in Weyl semimetals and the chiral anomaly, *Phys. Rev. B*

¹¹ In lattice gauge theory (for a compact gauge field), the gauge fixing is unnecessarily [75], but in the lattice perturbation theory, the gauge fixing is required [78].

- 86**, 115133 (2012), [arXiv:1206.1868 \[cond-mat.mes-hall\]](#).
- [16] P. Sikivie, Experimental Tests of the Invisible Axion, *Phys. Rev. Lett.* **51**, 1415 (1983), [Erratum: *Phys. Rev. Lett.* **52**, 695 (1984)].
- [17] F. Wilczek, Two Applications of Axion Electrodynamics, *Phys. Rev. Lett.* **58**, 1799 (1987).
- [18] O. G. Kharlanov and V. C. Zhukovsky, Casimir effect within $D = 3 + 1$ Maxwell-Chern-Simons electrodynamics, *Phys. Rev. D* **81**, 025015 (2010), [arXiv:0905.3680 \[hep-th\]](#).
- [19] K. Fukushima, S. Imaki, and Z. Qiu, Anomalous Casimir effect in axion electrodynamics, *Phys. Rev. D* **100**, 045013 (2019), [arXiv:1906.08975 \[hep-th\]](#).
- [20] I. Brevik, Axion Electrodynamics and the Axionic Casimir Effect, *Universe* **7**, 133 (2021), [arXiv:2202.11152 \[hep-ph\]](#).
- [21] F. Canfora, D. Dudal, T. Oosthuysen, P. Pais, and L. Rosa, The Casimir effect in chiral media using path integral techniques, *JHEP* **09**, 095, [arXiv:2207.09175 \[hep-th\]](#).
- [22] T. Oosthuysen and D. Dudal, Interplay between chiral media and perfect electromagnetic conductor plates: Repulsive vs. attractive Casimir force transitions, *SciPost Phys.* **15**, 213 (2023), [arXiv:2301.12870 \[hep-th\]](#).
- [23] A. M. Favitta, I. H. Brevik, and M. M. Chaichian, Axion electrodynamics: Green's functions, zero-point energy and optical activity, *Annals Phys.* **455**, 169396 (2023), [arXiv:2302.13129 \[hep-th\]](#).
- [24] Y. Ema, M. Hazumi, H. Iizuka, K. Mukaida, and K. Nakayama, Zero Casimir force in axion electrodynamics and the search for a new force, *Phys. Rev. D* **108**, 016009 (2023), [arXiv:2302.14676 \[hep-ph\]](#).
- [25] I. Brevik, M. Chaichian, and A. M. Favitta, On the Axion Electrodynamics in a two-dimensional slab and the Casimir effect, [arXiv:2310.05575 \[hep-th\]](#).
- [26] Q.-D. Jiang and F. Wilczek, Chiral Casimir forces: Repulsive, enhanced, tunable, *Phys. Rev. B* **99**, 125403 (2019), [arXiv:1805.07994 \[cond-mat.mes-hall\]](#).
- [27] J. S. Høye and I. Brevik, Casimir force between ideal metal plates in a chiral vacuum, *Eur. Phys. J. Plus* **135**, 271 (2020), [arXiv:2002.01719 \[quant-ph\]](#).
- [28] A. G. Grushin and A. Cortijo, Tunable Casimir Repulsion with Three Dimensional Topological Insulators, *Phys. Rev. Lett.* **106**, 020403 (2011), [arXiv:1002.3481 \[cond-mat.mtrl-sci\]](#).
- [29] A. G. Grushin, P. Rodriguez-Lopez, and A. Cortijo, Effect of finite temperature and uniaxial anisotropy on the Casimir effect with three-dimensional topological insulators, *Phys. Rev. B* **84**, 045119 (2011), [arXiv:1102.0455 \[cond-mat.mtrl-sci\]](#).
- [30] L. Chen and S. Wan, Casimir interaction between topological insulators with finite surface band gap, *Phys. Rev. B* **84**, 075149 (2011), [arXiv:1105.3554 \[cond-mat.other\]](#).
- [31] Z. Babamahdi, V. B. Svetovoy, D. T. Yimam, B. J. Kooi, T. Banerjee, J. Moon, S. Oh, M. Enache, M. Stöhr, and G. Palasantzas, Casimir and electrostatic forces from Bi_2Se_3 thin films of varying thickness, *Phys. Rev. B* **103**, L161102 (2021).
- [32] W.-K. Tse and A. H. MacDonald, Quantized Casimir Force, *Phys. Rev. Lett.* **109**, 236806 (2012), [arXiv:1208.3786 \[cond-mat.mes-hall\]](#).
- [33] P. Rodriguez-Lopez and A. G. Grushin, Repulsive Casimir Effect with Chern insulators, *Phys. Rev. Lett.* **112**, 056804 (2014), [arXiv:1310.2470 \[cond-mat.mes-hall\]](#).
- [34] I. Fialkovsky, N. Khusnutdinov, and D. Vassilevich, Quest for Casimir repulsion between Chern-Simons surfaces, *Phys. Rev. B* **97**, 165432 (2018), [arXiv:1802.06598 \[cond-mat.mes-hall\]](#).
- [35] J. H. Wilson, A. A. Allocca, and V. Galitski, Repulsive casimir force between weyl semimetals, *Phys. Rev. B* **91**, 235115 (2015), [arXiv:1501.07659 \[cond-mat.mes-hall\]](#).
- [36] P. Rodriguez-Lopez, A. Popescu, I. Fialkovsky, N. Khusnutdinov, and L. M. Woods, Signatures of Complex Optical Response in Casimir Interactions of Type I and II Weyl Semimetals, *Commun. Mater.* **1**, 14 (2020), [arXiv:1911.03377 \[cond-mat.mtrl-sci\]](#).
- [37] L. Chen and K. Chang, Chiral-Anomaly-Driven Casimir-Lifshitz Torque between Weyl Semimetals, *Phys. Rev. Lett.* **125**, 047402 (2020).
- [38] M. B. Farias, A. A. Zyuzin, and T. L. Schmidt, Casimir force between Weyl semimetals in a chiral medium, *Phys. Rev. B* **101**, 235446 (2020), [arXiv:2001.10329 \[cond-mat.mes-hall\]](#).
- [39] M. Bordag, I. Fialkovsky, N. Khusnutdinov, and D. Vassilevich, Bulk contributions to the Casimir interaction of Dirac materials, *Phys. Rev. B* **104**, 195431 (2021), [arXiv:2107.10369 \[cond-mat.mes-hall\]](#).
- [40] J.-N. Rong, L. Chen, and K. Chang, Chiral Anomaly-Enhanced Casimir Interaction between Weyl Semimetals, *Chin. Phys. Lett.* **38**, 084501 (2021).
- [41] L. M. Woods, D. A. R. Dalvit, A. Tkatchenko, P. Rodriguez-Lopez, A. W. Rodriguez, and R. Podgornik, Materials perspective on Casimir and van der Waals interactions, *Rev. Mod. Phys.* **88**, 045003 (2016), [arXiv:1509.03338 \[cond-mat.mtrl-sci\]](#).
- [42] B.-S. Lu, The Casimir Effect in Topological Matter, *Universe* **7**, 237 (2021), [arXiv:2105.11059 \[cond-mat.mes-hall\]](#).
- [43] A. Actor, I. Bender, and J. Reingruber, Casimir effect on a finite lattice, *Fortschr. Phys.* **48**, 303 (2000), [arXiv:quant-ph/9908058 \[quant-ph\]](#).
- [44] M. Pawellek, Finite-sites corrections to the Casimir energy on a periodic lattice, [arXiv:1303.4708 \[hep-th\]](#).
- [45] T. Ishikawa, K. Nakayama, and K. Suzuki, Casimir effect for lattice fermions, *Phys. Lett. B* **809**, 135713 (2020), [arXiv:2005.10758 \[hep-lat\]](#).
- [46] T. Ishikawa, K. Nakayama, and K. Suzuki, Lattice-fermionic Casimir effect and topological insulators, *Phys. Rev. Res.* **3**, 023201 (2021), [arXiv:2012.11398 \[hep-lat\]](#).
- [47] K. Nakayama and K. Suzuki, Remnants of the nonrelativistic Casimir effect on the lattice, *Phys. Rev. Res.* **5**, L022054 (2023), [arXiv:2204.12032 \[quant-ph\]](#).
- [48] K. Nakata and K. Suzuki, Magnonic Casimir Effect in Ferrimagnets, *Phys. Rev. Lett.* **130**, 096702 (2023), [arXiv:2205.13802 \[quant-ph\]](#).
- [49] Y. V. Mandlecha and R. V. Gavai, Lattice fermionic Casimir effect in a slab bag and universality, *Phys. Lett. B* **835**, 137558 (2022), [arXiv:2207.00889 \[hep-lat\]](#).
- [50] K. Nakayama and K. Suzuki, Dirac/Weyl-node-induced oscillating Casimir effect, *Phys. Lett. B* **843**, 138017 (2023), [arXiv:2207.14078 \[cond-mat.mes-hall\]](#).
- [51] B. Swingle and M. Van Raamsdonk, Enhanced negative energy with a massless Dirac field, *JHEP* **08**, 183, [arXiv:2212.02609 \[hep-th\]](#).
- [52] K. Nakata and K. Suzuki, Non-Hermitian Casimir Effect of Magnons, [arXiv:2305.09231 \[quant-ph\]](#).
- [53] O. Pavlovsky and M. Ulybyshev, Casimir energy cal-

- culations within the formalism of the noncompact lattice QED, *Int. J. Mod. Phys. A* **25**, 2457 (2010), [arXiv:0911.2635 \[hep-lat\]](#).
- [54] O. V. Pavlovsky and M. V. Ulybyshev, Casimir energy in noncompact lattice electrodynamics, *Theor. Math. Phys.* **164**, 1051 (2010), [*Teor. Mat. Fiz.* **164**, 262 (2010)].
- [55] O. Pavlovsky and M. Ulybyshev, Monte-Carlo calculation of the lateral Casimir forces between rectangular gratings within the formalism of lattice quantum field theory, *Int. J. Mod. Phys. A* **26**, 2743 (2011), [arXiv:1105.0544 \[quant-ph\]](#).
- [56] O. Pavlovsky and M. Ulybyshev, Casimir energy in the compact QED on the lattice, [arXiv:0901.1960 \[hep-lat\]](#).
- [57] M. N. Chernodub, V. A. Goy, and A. V. Molochkov, Casimir effect on the lattice: U(1) gauge theory in two spatial dimensions, *Phys. Rev. D* **94**, 094504 (2016), [arXiv:1609.02323 \[hep-lat\]](#).
- [58] M. N. Chernodub, V. A. Goy, and A. V. Molochkov, Nonperturbative Casimir effect and monopoles: compact Abelian gauge theory in two spatial dimensions, *Phys. Rev. D* **95**, 074511 (2017), [arXiv:1703.03439 \[hep-lat\]](#).
- [59] M. N. Chernodub, V. A. Goy, and A. V. Molochkov, Casimir effect and deconfinement phase transition, *Phys. Rev. D* **96**, 094507 (2017), [arXiv:1709.02262 \[hep-lat\]](#).
- [60] M. N. Chernodub, V. A. Goy, A. V. Molochkov, and A. S. Tanashkin, Casimir boundaries, monopoles, and deconfinement transition in $(3 + 1)$ - dimensional compact electrodynamics, *Phys. Rev. D* **105**, 114506 (2022), [arXiv:2203.14922 \[hep-lat\]](#).
- [61] M. N. Chernodub, V. A. Goy, A. V. Molochkov, and H. H. Nguyen, Casimir Effect in Yang-Mills Theory in $D = 2 + 1$, *Phys. Rev. Lett.* **121**, 191601 (2018), [arXiv:1805.11887 \[hep-lat\]](#).
- [62] M. N. Chernodub, V. A. Goy, and A. V. Molochkov, Phase structure of lattice Yang-Mills theory on $\mathbb{T}^2 \times \mathbb{R}^2$, *Phys. Rev. D* **99**, 074021 (2019), [arXiv:1811.01550 \[hep-lat\]](#).
- [63] M. Kitazawa, S. Mogliacci, I. Kolbé, and W. A. Horowitz, Anisotropic pressure induced by finite-size effects in SU(3) Yang-Mills theory, *Phys. Rev. D* **99**, 094507 (2019), [arXiv:1904.00241 \[hep-lat\]](#).
- [64] M. N. Chernodub, V. A. Goy, A. V. Molochkov, and A. S. Tanashkin, Boundary states and non-Abelian Casimir effect in lattice Yang-Mills theory, *Phys. Rev. D* **108**, 014515 (2023), [arXiv:2302.00376 \[hep-lat\]](#).
- [65] A. Vilenkin, Equilibrium parity-violating current in a magnetic field, *Phys. Rev. D* **22**, 3080 (1980).
- [66] H. B. Nielsen and M. Ninomiya, The Adler-Bell-Jackiw anomaly and Weyl fermions in a crystal, *Phys. Lett. B* **130**, 389 (1983).
- [67] D. Kharzeev, Parity violation in hot QCD: Why it can happen, and how to look for it, *Phys. Lett. B* **633**, 260 (2006), [arXiv:hep-ph/0406125](#).
- [68] D. Kharzeev and A. Zhitnitsky, Charge separation induced by P-odd bubbles in QCD matter, *Nucl. Phys. A* **797**, 67 (2007), [arXiv:0706.1026 \[hep-ph\]](#).
- [69] D. E. Kharzeev, L. D. McLerran, and H. J. Warringa, The Effects of topological charge change in heavy ion collisions: 'Event by event P and CP violation', *Nucl. Phys. A* **803**, 227 (2008), [arXiv:0711.0950 \[hep-ph\]](#).
- [70] K. Fukushima, D. E. Kharzeev, and H. J. Warringa, Chiral magnetic effect, *Phys. Rev. D* **78**, 074033 (2008), [arXiv:0808.3382 \[hep-ph\]](#).
- [71] E. Witten, Dyons of Charge $e\theta/2\pi$, *Phys. Lett. B* **86**, 283 (1979).
- [72] E. M. Lifshitz, The theory of molecular attractive forces between solids, *Sov. Phys. JETP* **2**, 73 (1956).
- [73] J. Ambjørn and S. Wolfram, Properties of the vacuum. I. Mechanical and thermodynamic, *Annals Phys.* **147**, 1 (1983).
- [74] A. C. Aguiar Pinto, T. M. Britto, R. Bunchaft, F. Pascoal, and F. S. S. da Rosa, Casimir effect for a massive scalar field under mixed boundary conditions, *Braz. J. Phys.* **33**, 860 (2003).
- [75] K. G. Wilson, Confinement of quarks, *Phys. Rev. D* **10**, 2445 (1974).
- [76] M. E. Peskin, *Chirality conservation in the lattice gauge theory*, Ph.D. thesis, Cornell University (1978).
- [77] P. Di Vecchia, K. Fabricius, G. C. Rossi, and G. Veneziano, Preliminary evidence for $U_A(1)$ breaking in QCD from lattice calculations, *Nucl. Phys. B* **192**, 392 (1981).
- [78] S. Capitani, Lattice perturbation theory, *Phys. Rep.* **382**, 113 (2003), [arXiv:hep-lat/0211036](#).